Clim Dyn
DOI 10.1007/s00382-009-0700-y

The 1983 drought in the West Sahel: a case study

Jürgen Bader · Mojib Latif

Received: 3 June 2009 / Accepted: 27 October 2009

Abstract Some drought years over sub-Saharan west Africa (1972, 1977, 1984) have been previously related to a cross-equatorial Atlantic gradient pattern with anomalously warm sea surface temperatures (SSTs) south of 10°*N* and anomalously cold SSTs north of 10°*N*. This SST dipole-like pattern was not characteristic of 1983, the third driest summer of the twentieth century in the Sahel. This study presents evidence that the dry conditions that persisted over the west Sahel in 1983 were mainly forced by high Indian Ocean SSTs that were probably remanent from the strong 1982/1983 El Niño event. The synchronous Pacific impact of the 1982/1983 El Niño event on west African rainfall was however, quite weak. Prior studies have mainly suggested that the Indian Ocean SSTs impact the decadal-scale rainfall variability over the west Sahel. This study demonstrates that the Indian Ocean also significantly affects inter-annual rainfall variability over the west Sahel and that it was the main forcing for the drought over the west Sahel in 1983.

Keywords Sahel · Drought · Rainfall · SST · Indian Ocean

J. Bader (✉)
Bjerknes Centre for Climate Research,
Allégaten 70, 5007 Bergen, Norway
e-mail: juergen.bader@bjerknes.uib.no

J. Bader
Geophysical Institute, University of Bergen,
Bergen, Norway

M. Latif
Leibniz-Institute for Marine Sciences
at the University of Kiel, Kiel, Germany

1 Introduction

Many studies have documented the existence of strong inter-annual to decadal-scale rainfall variability over sub-Saharan west Africa (Ward et al. 1999). Since the early 1970s, sub-Saharan west-Africa has suffered from a prolonged drought that has/had large, mostly negative, impacts on agriculture, industrial development, human health, and hydro-power production. The prolonged drought has also caused migration problems. Better predictions of the west African monsoon and better understanding of its sensitivity to various forcings could have large social and economic benefits if used to help ameliorate some of these drought impacts.

The causes of sub-Saharan west Africa rainfall variability are not been completely understood, but observational and model-based studies show that rainfall variability is associated with regional and global SST anomaly patterns. SST anomalies in the Atlantic (Lamb 1978a, b; Hastenrath 1984; Lamb and Peppler 1992; Ward 1998; Vizy and Cook 2001, 2002), in the Pacific (Janicot 1996; Rowell 2001), in the Indian Ocean (Palmer 1986; Shinoda and Kawamura 1994; Bader and Latif 2003; Lu and Delworth 2005), and in the Mediterranean (Rowell 2003) have all been shown to have a demonstrable impact. Folland et al. (1986) linked near global changes in sea surface temperatures (SSTs) to Sahelian rainfall variability. The anomalies include relative changes in SST between the hemispheres. Lamb (1978a, b) and Lamb and Peppler (1992) presented case studies of tropical Atlantic atmospheric and oceanic conditions during the sub-Saharan-deficient rainy seasons 1972, 1977, 1983, 1984. One of their key result for the drought years 1972, 1977, 1984 included a distinctive basin-wide Atlantic cross-equatorial SST gradient pattern with warm

Published online: 12 November 2009

anomalies to the south of 10°*N* and cold anomalies between 10°*N* and 25°*N*. The role of the SST dipole-like pattern in the tropical Atlantic in causing extremely deficient rainfall over the Sahel was also confirmed by Palmer (1986). The third largest summer drought in 1983 was not associated with a similar Atlantic SST dipole-like pattern (Lamb and Peppler 1992).

Given that the Atlantic SST gradient does not appear to be the dominant forcing of the negative rainfall anomalies over the west Sahel in 1983, a possible alternative is the eastern tropical Pacific SST anomalies associated with the 1982/1983 El Niño. Studies by Janicot (1996) and Rowell (2001) linked positive tropical Pacific SSTs to drought conditions in the Sahel. We will assess the role of tropical SST anomalies in forcing the 1983 rainfall anomalies over west Africa by analysing observational/reanalysis data and the output of ensemble experiments with an atmospheric general circulation model (AGCM).

2 Observational data

Two observational rainfall data-sets are used. One is the gauge based CRU TS 2.1 data-set (Mitchell and Jones 2005). It is a land-only global, gridded, monthly data-set. The spatial resolution is 0.5° × 0.5°. It covers the period 1901–2002. The second rainfall set is the global, monthly CPC Merged Analysis of Precipitation (CMAP) data-set (Xie and Arkin 1996). Values are obtained from five kinds of satellite estimates (GPI, OPI, SSM/I scattering, SSM/I emission and MSU). The data is 2.5° × 2.5° gridded and covers the period 1979–2005. The SSTs used in this study are the HadISST1.1 SSTs (Rayner et al. 2003). It is a global, gridded, monthly SST data-set in 1° × 1° spatial resolution and its temporal coverage is from 1870 to present. The NCEP/NCAR Reanalysis data (Kalnay et al. 1996) is used for the wind fields and was provided by the NOAA/OAR/ESRL PSD, Boulder, CO, USA, from their Web site at http://www.cdc.noaa.gov/. The analysis will mainly focus on the boreal summer season July–September (JAS). Anomalies are computed relative to the Atmospheric Model Intercomparison Project II (AMIP2) climatology period (January 1979–February 1996). Several indices have been defined. The west Sahel is defined from the west coast to 10°*E* and from 12°*N* to 20°*N* (see marked region in Fig. 2a). The NINO3-region in the Pacific is the area-average from 90°*W* to 150°*W* and from 5°*S* to 5°*N* and the eastern tropical Atlantic region from 10°*W* to the west coast of Africa and from 10°*S* northward to the coast of Guinea. The Indian Ocean index is computed from the east coast of Africa to 120°*E* and from 30°*S* northward to the south coast of Asia.

3 Observations

Figure 1 shows the annual cycle of observed (CRU) precipitation over the west Sahel. The rainfall over the west Sahel is strongly seasonally dependent in both the observations and in the model output. Most of the annual rainfall occurs during summer. Rainfall over the west Sahel is associated with south-westerly monsoonal winds that blow from the tropical Atlantic to west Africa (Fig. 2a). Smaller rainfall amounts occur in the adjacent surrounding months (May, June and October).

Figure 3 shows the area-averaged summer (JAS) rainfall anomaly over the west Sahel based on the CRU data-set. The drying trend from the 1950s to the mid-1980s is evident with some recovery toward climatology in the years since the mid-1980s. 1983 was an extremely dry year in the west Sahel. Figure 4 shows a map of the 1983 summer precipitation anomaly in the CMAP data-set relative to the climatological mean. During the summer of 1983, the rainfall was substantially below average over sub-Saharan west Africa. The rainfall over the Indian Ocean was exceptionally high. Figure 5 shows the observed SST anomalies during the summer of 1983 relative to the AMIP2 climatology period (1979–1995) using the Hadley-SST-data-set. The SSTs in the eastern tropical Pacific were warmer than normal during the summer of 1983 and have a

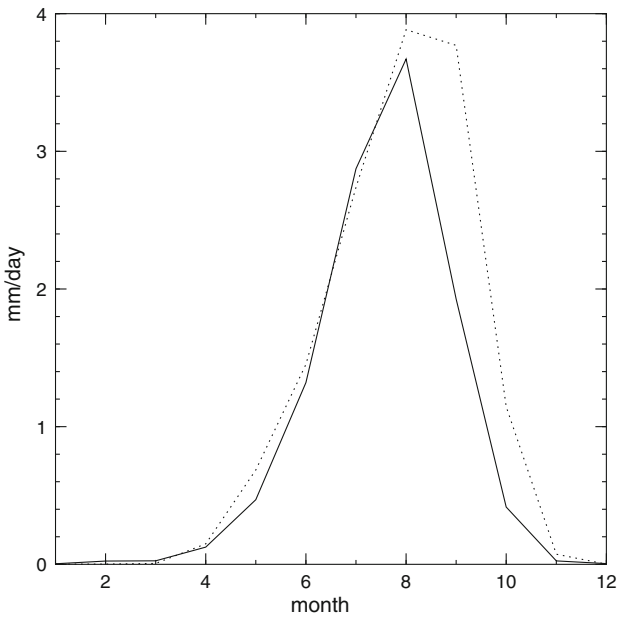

Fig. 1 Annual cycle of precipitation averaged over the west Sahel (mm/day). The west Sahel index is computed over the region from 15°*W* to 10°*E* and from 12°*N* to 20°*N*. The *solid curve* shows the observed seasonal cycle and the *dotted curve* the simulated seasonal cycle by ECHAM5. The observation is based on the CRU data-set and the simulated is based on our control integration. For better comparision the seasonal cycle for the observations is computed over the period 1979–1995

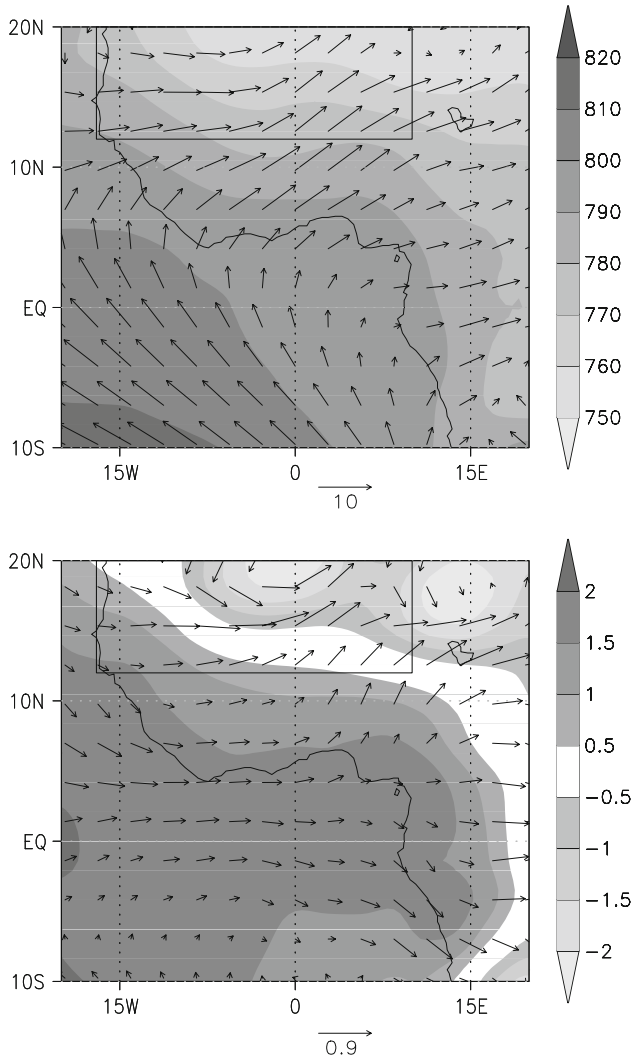

Fig. 2 Upper figure shows the simulated summer (JAS) horizontal wind [vectors (m/s)] and the geopotential height [shading (gpm)] in our control integration in 925 hPa. *Lower* horizontal wind (m/s) and geopotential height response (gpm) of the Indian ocean experiment (Indian ocean experiment minus control integration)

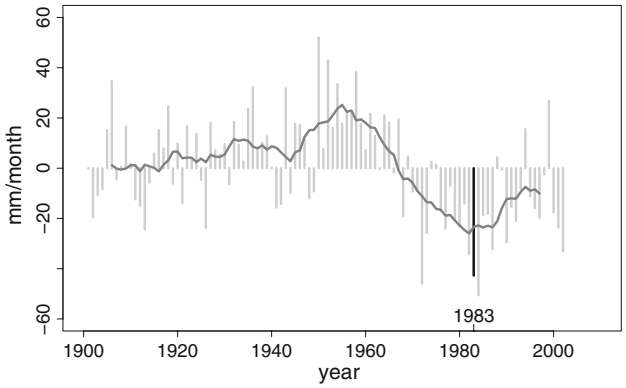

Fig. 3 observed summer (JAS) rainfall anomaly over the western Sahel (see text for details) based on the CRU data-set (mm/month). *Grey bars* indicate seasonal means, the line the 11-year running mean of the summer rainfall and the *black bar* indicates the rainfall anomaly in the year 1983

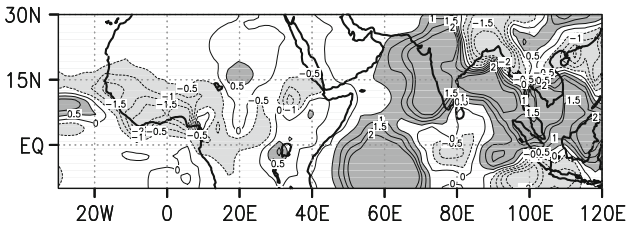

Fig. 4 Observed JAS precipitation anomaly during 1983 relative to the climatological mean (1979–1996), based on the CMAP data-set (mm/day)

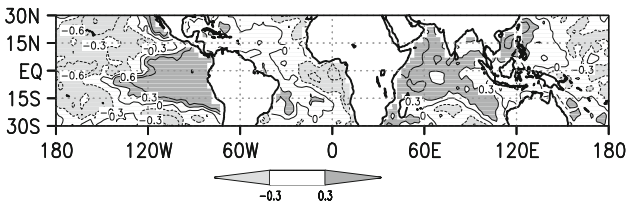

Fig. 5 Observed JAS SST anomaly in the tropics during 1983 relative to the climatological mean (1979–1995) based on the Hadley SST data-set (Kelvin)

spatial pattern characteristic of an El Niño. Figure 6 shows the time-series for the NINO3-index in the eastern tropical Pacific for (a) the summer (JAS) and (b) winter (DJF) season. Eastern tropical Pacific SSTs were warmer than normal during summer 1983 but not exceptional (Fig. 6a). The central Pacific has already cooled (Fig. 5). Tropical Pacific 1982/1983 winter (December–February) SSTs in the NINO3 region are the second warmest in the period of the Hadley SST data-set (Fig. 6b).

1983 summer SSTs in the tropical Atlantic do not show the cross-equatorial SST-gradient pattern characteristic for the Sahelian droughts in 1972, 1977 and 1984 (Lamb 1978a, b; Palmer 1986, Lamb and Peppler 1992). The SSTs in the eastern tropical Atlantic near the Guinea Coast were colder in the summer of 1983 compared to the 1979 to 1995 reference period. The 1983 summer SSTs in the tropical north Atlantic were not strongly anomalous (Fig. 5). Figure 6c shows time series of average eastern tropical Atlantic SSTs during summer 1983. The eastern tropical Atlantic shows a warming trend in recent decades. The SSTs were colder than normal during the summer of 1983, but were not exceptionally.

The 1983 summer SSTs in the Indian Ocean were exceptionally warm (Fig. 6d). The Indian ocean summer SSTs show a warming trend since the 1950s. Even after removing the general warming trend in the Indian Ocean the 1983 SSTs stand out as a significant inter-annual anomaly. The 1983 summer SSTs in the Indian Ocean were the third warmest during the 1870–2005. It is likely that the strong

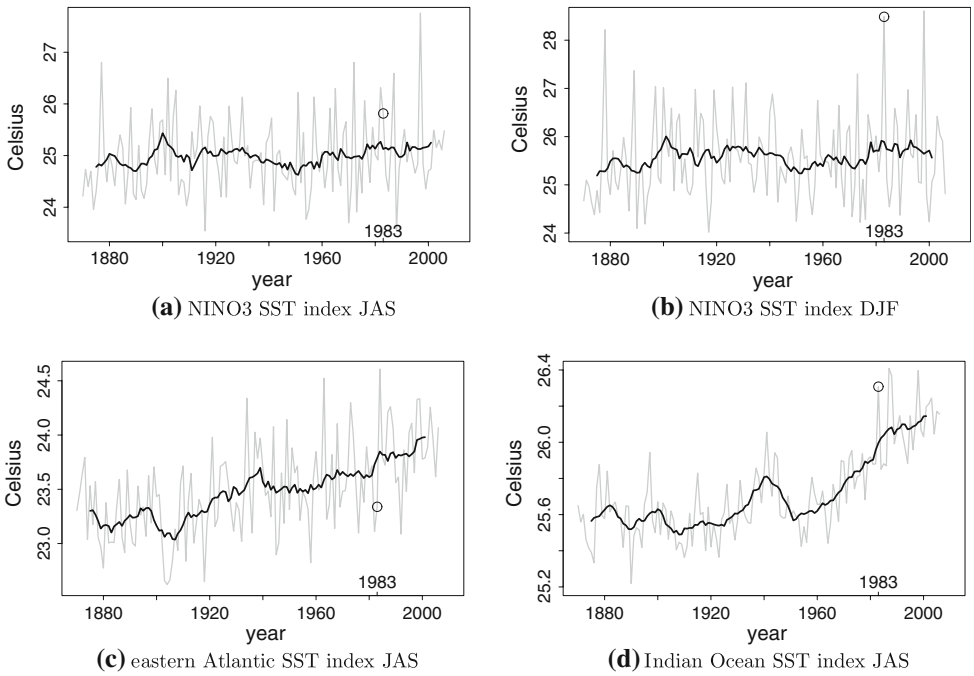

Fig. 6 **a** Observed summer (JAS) and **b** winter (DJF) NINO3-SST-index, **c** observed summer (JAS) eastern tropical Atlantic SST-index; **d** observed summer (JAS) Indian Ocean SST-index. The *grey curves* denote seasonal values the black curves an 11-year running mean. The year 1983 is marked by a *circle*. The data is based on the Hadley SST data-set (Celsius)

Indian Ocean SST anomalies observed during the summer 1983 were forced remotely by the SST anomalies in the Pacific during the strong El Niño event 1982/1983 (Tourre and White 1995; Chiang and Sobel 2002; Figs. 5, 6b). An analysis of the origin of the Indian Ocean SST anomalies is considered to be beyond the scope of this paper.

4 Model/experiments

The role of the different SST anomalies in the tropical Atlantic, Indian and Pacific Ocean basins in determining sub-Saharan west African rainfall during summer 1983 is investigated by means of an ensemble of atmospheric model experiments. The model used in this case study is the global AGCM ECHAM5 (Roeckner et al. 2006). A substantially more detailed description of the model ECHAM5 is given in a technical report (Roeckner et al. 2003). The atmospheric model is run at T42 ($\approx 2.8° \times 2.8°$) horizontal resolution with 19 vertical levels. The 12 observed monthly SST fields of the year 1983 were prescribed in different ocean basins: the tropical Atlantic, the tropical Indian, the tropical Pacific, and both the tropical Atlantic and Indian Oceans (Fig. 7). In all other ocean areas the climatological AMIP2 SSTs are used. The SST anomalies in the tropics are obtained from the Hadley-SST-data-set (Rayner et al. 2003). All other external forcings (e.g. greenhouse gases, solar radiation) are the same for all integrations. The experimental setup of the individual simulations differs only in the SST forcing. Results are obtained from a set of 21-year long SST sensitivity

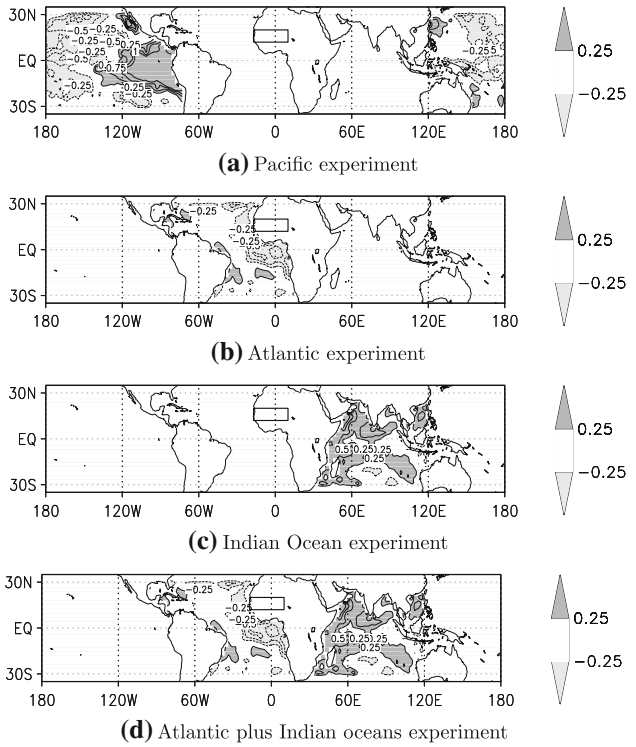

Fig. 7 The four SST anomaly patterns used in the response experiments (Kelvin). **a** The Atlantic part, **b** the Indian Ocean part, **c** the Pacific part, and **d** the Atlantic-Indian Ocean SST anomaly observed during the JAS period 1983

experiments. The results are averaged over the last twenty years and only the mean July–September (JAS) response (sensitivity run minus control integration) is shown here.

A 20-year control simulation forced by the AMIP2 climatological SSTs serves as the reference run. Figure 1 shows the annual cycle of the observed and simulated precipitation over the west Sahel. The solid line shows the observations (CRU) and the dotted line the simulated west Sahel rainfall from the control integration. The model (dotted curve) reproduces the observed annual cycle (solid curve) reasonably well. The simulated precipitation curve matches the observations well during spring and summer and reproduces the rainfall maximum in August. The model overestimates the rainfall in late summer/autumn, especially in September.

AGCMs (including ECHAM5) tend to underestimate the interannual and decadal rainfall variability over west Africa (Schnitzler et al. 2001; Giannini et al. 2003). This might be due to the coarse resolution of the models and/or because of missing or inaccurately parametrised physical features like dynamic vegetation and convection. Zeng et al. (1999) showed that land surface feedback increases the precipitation variability over the Sahel on inter-annual and inter-decadal time-scales.

5 Results

Our first experiment is performed by forcing the model by the Pacific SST anomalies only (Fig. 7a). The experiment does not show a clear direct (via the atmosphere) impact on sub-Saharan west Africa rainfall in response to SST anomalies in the tropical Pacific during summer 1983 (Fig. 8a). The rainfall anomalies that result from the Pacific SST forcing have the opposite sign than those observed over most regions of sub-Saharan west Africa. Strong tropical precipitation and circulation responses are limited to the equatorial Pacific Ocean which is characterized by a sharp east-west SST-gradient.

The second SST sensitivity experiment is forced by Atlantic SST anomalies of 1983 (Fig. 7b). The Atlantic SST anomalies in 1983 are characterised by cold SST anomalies in the eastern tropical Atlantic region, but the cross-equatorial SST gradient pattern characteristic of other extremely dry years in the Sahel (Lamb 1978a, b; Palmer 1986; Lamb and Peppler 1992) is absent. The model's rainfall response (mm/day) to Atlantic SST anomalies shows a significant rainfall reduction along the Guinea Coast at the 95%-confidence-level according to a two-tailed t test (Fig. 8b, significance is indicated by shading). The response of west African rainfall is mainly restricted along the Guinea Coast and there is no clear response in rainfall over the west Sahel. Figure 9 shows the corresponding response of horizontal moisture divergence in a latitude-height cross-section averaged from 15°W to 10°E. There is a significant reduction in moisture

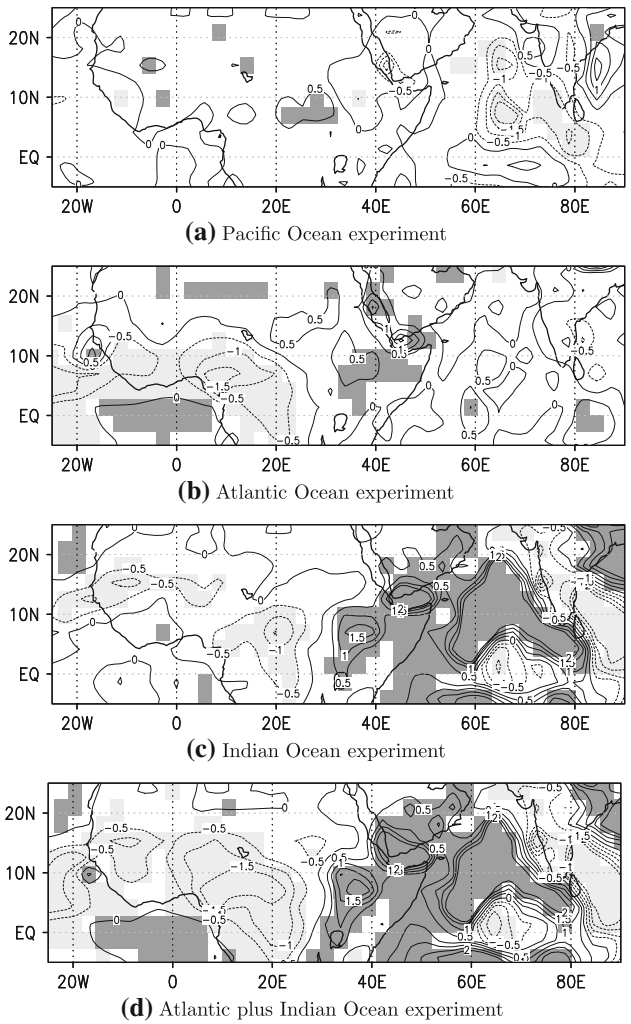

Fig. 8 Simulated summer (JAS) rainfall anomaly pattern (mm/day) for **a** the Pacific Ocean experiment, **b** the Atlantic Ocean experiment, **c** the Indian Ocean experiment, **d** the Atlantic plus Indian Ocean experiment. Shown are anomalies relative to the control integration forced by climatological SSTs. Values that exceed the 95% significance level according to a two-tailed t test are *shaded light* for negative anomalies and *dark* for positive. The contour interval is 0.5 mm/day

convergence in the boundary layer along Guinea Coast. A significant reduction in the vertically integrated specific humidity (precipitable water) is simulated in the source region for rainfall associated with the west African monsoon—the tropical Atlantic—and along Guinea Coast (Fig. 10). A reduction in evaporation (not shown) due to the colder SSTs in the eastern tropical Atlantic seem to be the main cause of the reduction in precipitable water in the boundary layer over the tropical Atlantic (not shown). The reduction in precipitable water along the Guinea Coast is associated with a reduced humidity flux from the tropical Atlantic to west Africa (Fig. 10). The experiment indicates that reduction of moisture transport by the monsoon circulation is the main cause of the rainfall reduction along

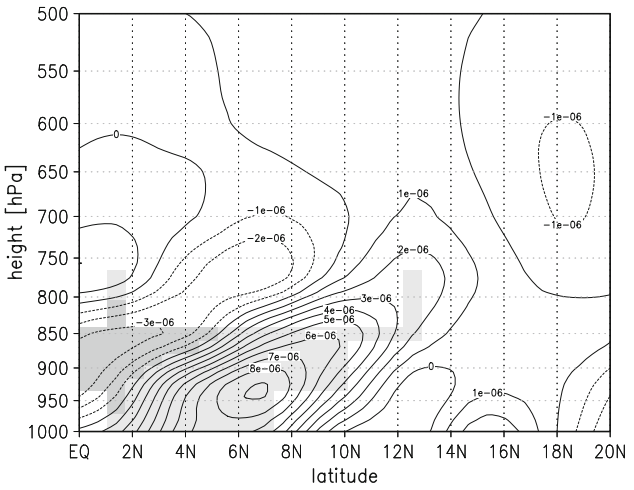

Fig. 9 Height-latitude cross-section of the response in simulated horizontal moisture divergence averaged from 15°*W* to 10°*E* for the Atlantic experiment [g/(kg s)]. Shown are anomalies relative to the control integration forced by climatological SSTs. Only significant changes in horizontal moisture divergence at the 95% significance level according to a two-tailed *t* test are *shaded*. *Dashed contours* represent negative values of the horizontal moisture divergence and *solid lines* positive: *dashed curves* mean moisture convergence and solid moisture divergence

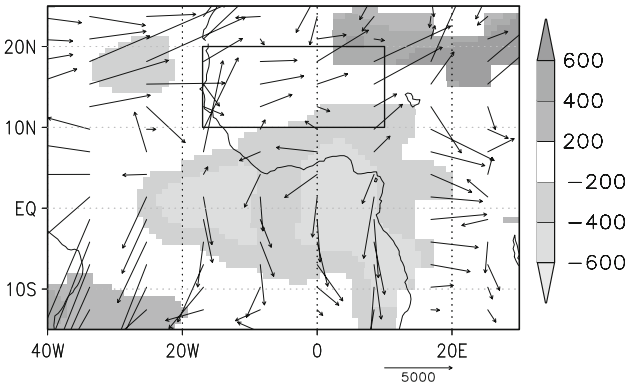

Fig. 10 Response in simulated vertically integrated specific humidity (precipitable water) in kg/m^2 and vertically integrated humidity flux in mg/(skg) for the Atlantic experiment. Shown are anomalies relative to the control integration forced by climatological SSTs. Only significant changes in precipitable water at the 95% significance level according to a two-tailed *t* test are *shaded*. The *vectors* show the response in the vertically integrated humidity flux

Guinea Coast. However, the impact of the 1983 tropical Atlantic SST anomalies seems to be mainly limited to the coastal region extending up to 10°*N*.

In the third experiment, the forcing is restricted to the tropical Indian Ocean (Fig. 7c). The warmer Indian Ocean SSTs during the summer 1983 lead to strong positive rainfall anomalies over the Indian Ocean (Fig. 8c). This is in general agreement with the observations (Fig. 4), confirming a relationship between warm SSTs and more rainfall over the Indian Ocean in the model during the summer of 1983. Significant rainfall reductions are simulated over the west Sahel (Fig. 8c). The computed area-averaged west-Sahel rainfall index—indicated by the box in Fig. 2—shows a significant reduction over the west Sahel at the 95% confidence level according to a two-tailed *t* test. The large-scale response to the warming in the Indian Ocean is a stationary equatorial Rossby-wave-like-pattern in the upper troposphere centred over the western Indian Ocean. Figure 11a shows the 200 hPa eddy stream-function response of the Indian Ocean experiment relative to our control integration and Fig. 11b the 850 hPa eddy stream-function response. The eddy stream-function is defined as the deviation from the zonal mean. The 850 hPa pattern shows a quadrupole response with two cyclones over Africa and two anti-cyclones over the Indian Ocean. The upper troposphere pattern is more or less reversed—although less clear than the lower tropospheric pattern—indicating a baroclinic response. This response is similar to the one found by Rowell (2001), where a stationary equatorial Rossby wave-like pattern was forced by convective heating anomalies over the Indian Ocean. Figure 12 shows the simulated summer anomalies in horizontal winds and horizontal divergence in 200 hPa in the Indian Ocean experiment, which suggests an association of the simulated rainfall enhancement over the Indian Ocean and eastern Africa with divergence in the upper troposphere. The upper tropospheric velocity potential response shows the center of the anomalous divergent flow over the western Indian Ocean (not shown). The figure also shows anomalous

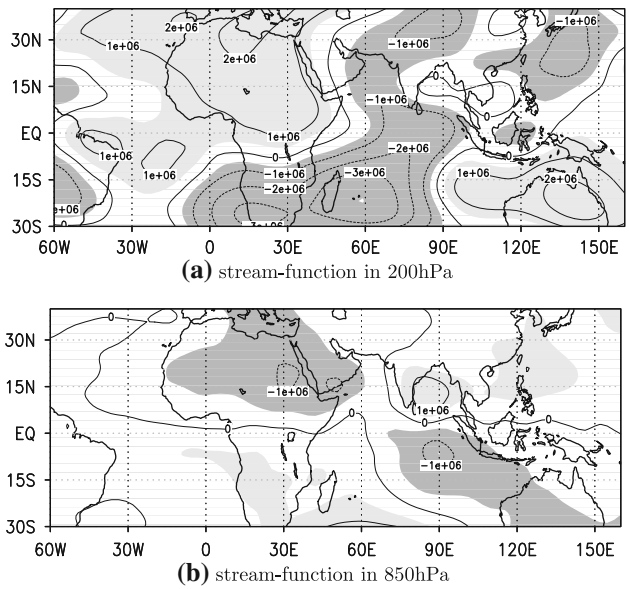

Fig. 11 The summer JAS 200hPa and 850hPa stream-function anomaly patterns (m^2/s) for the Indian Ocean experiment. Shown are the simulated anomalies relative to the control integration forced by climatological SSTs. *Light shading* indicates anomalies exceeding 5×10^5 and *dark shading* represents anomalies lower than -5×10^5

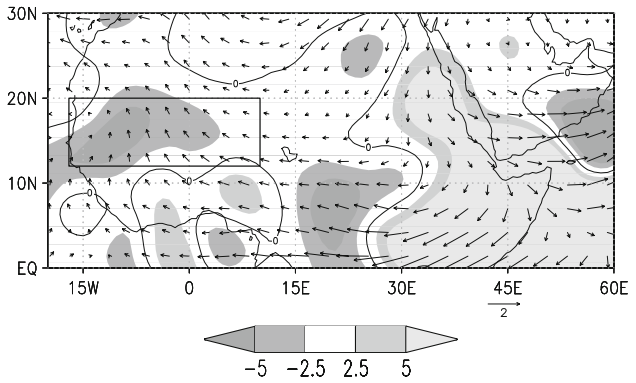

Fig. 12 The summer JAS 200 hPa wind anomaly pattern indicated by the *vectors* (m/s) and the anomalous horizontal divergence (1/s) for the Indian Ocean experiment experiment. Shown are the simulated anomalies relative to the control integration forced by climatological SSTs

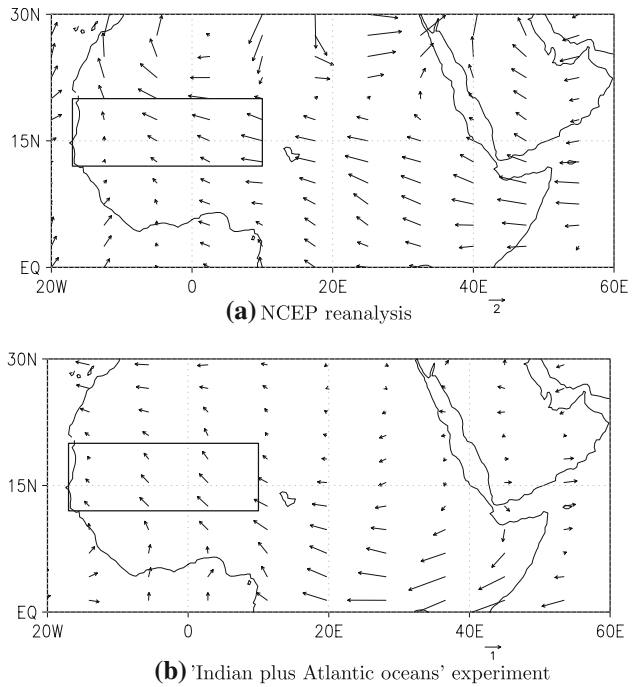

Fig. 13 **a** The 1983 summer JAS 200 hPa horizontal wind anomaly pattern in the NCEP reanalysis data (m/s). Shown are the anomalies in 1983 relative to the climatological means over the period 1979–1995. **b** The summer JAS 200hPa horizontal wind anomaly pattern for the 'Indian plus Atlantic oceans' experiment (m/s)

200hPa winds that are predominantly easterly or south-easterly blowing from the Indian Ocean to the west Sahel, which is similar to the south-easterly wind anomaly pattern, observed in the NCEP-NCAR reanalysis data during the summer of 1983 (Fig. 13). The Indian Ocean experiment underestimates the magnitude of the wind anomalies substantially. The horizontal wind anomalies converge over Africa west of approximately 25°*E* in the upper troposphere (Fig. 12). Figure 14 shows anomalies in the Indian Ocean

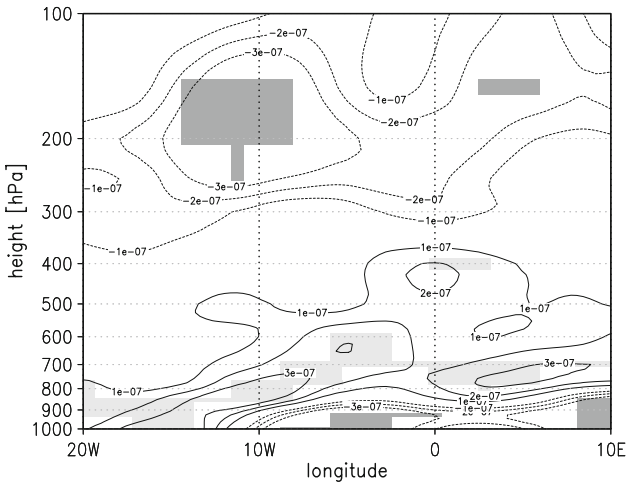

Fig. 14 Cross section of the summer (JAS) horizontal wind divergence anomalies averaged from 12°*N* to 20°*N* for the Indian Ocean experiment (1/s). The xaxis shows the longitude and the y-axis the height. The *contours* indicate the horizontal divergence. *Positive values* mean divergence and *negative* convergence. The *shading* denotes significant changes at the 95% significance level according to a two-tailed *t* test

experiment of the summer horizontal wind divergence averaged over a west African cross-section from 12°*N* to 20°*N*. The horizontal wind anomalies produce significant convergence over the west Sahel in the upper troposphere centred approximately at the 200 hPa level. The convergence in the upper troposphere leads to large scale anomalous subsidence below the maximum convergence due to continuity (Fig. 15). Large scale anomalous subsidence suppresses convection by increasing the stability due to adiabatic warming in the troposphere. The NCEP reanalysis data show indeed reduced ascent over west Africa during the summer of 1983 compared to climatology (1979–1995) confirming our model results (not shown). Figure 15 shows a longitude-height cross-section of the summer 1983 zonal and vertical wind anomalies along the line—shown in the upper panel—in the Indian Ocean experiment. It indicates a thermally driven circulation with upward motion over the Indian ocean/east Africa, easterly winds in the upper troposphere and downward motion over the west Sahel. The return flow from the west Sahel toward the east is not at the surface but is centred around the 800 hPa level, approximately at the level of the African Easterly Jet (AEJ). The circulation response is similar to the Indian Ocean forcing case studied by Lu (2009) using the GFDL model. The anomalous subsidence also does not extend to the surface over the west Sahel—the AEJ seems to be a barrier for the vertical motion. The reduction of the ascent is limited to the layer between the AEJ and the Tropical Easterly Jet (TEJ). Nicholson (2009) developed a revised version of the dynamics of the monsoon circulation over west Africa by analysing the NCEP reanalysis data, finding that the

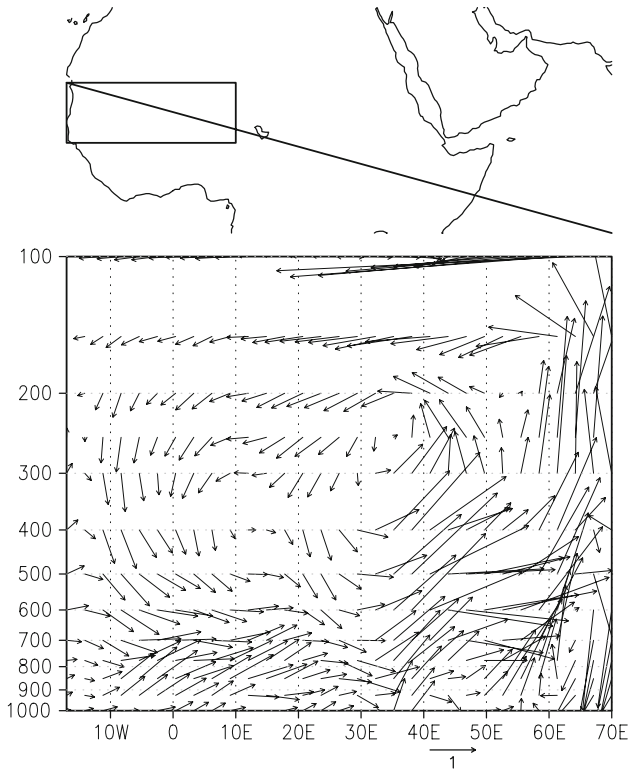

Fig. 15 Cross-section of the summer (JAS) zonal-vertical wind response for the Indian Ocean experiment (Indic experiment minus control integration) along the line shown in the upper figure. The vertical wind anomaly (omega) has been scaled by a factor of −100. The units of the zonal wind is m/s and the vertical wind (omega) is in Pa/s

primary rain-producing mechanism over the Sahel is the core of ascent lying between the axes of the AEJ and TEJ. Our Indian Ocean experiment is consistent with this view. The impact of the Indian Ocean warming reduces the uplift at these levels. Anomalous westerly winds concentrated at the level of the AEJ may cause ascent below this level over the west Sahel (Fig. 15). Anomalous upward motion is associated with anomalously low geopotential heights over the Sahel in the levels below the AEJ strengthening the horizontal geopotential height gradient between the tropical Atlantic and west Africa and leading to a stronger monsoonal circulation, especially from the west coast to Africa (see lower panel of Fig. 2). The enhancement of the monsoon circulation is associated with a local enhancement of precipitation along the western Guinea Coast. This causes a weak dipole-like rainfall anomaly pattern between the west Sahel and Guinea Coast with mid and upper tropospheric anomalous subsidence associated with Sahel drying and a near-surface enhancement of the monsoon leading to a wetter Guinea Coast. This dipole-like pattern is more pronounced in the precipitable water anomalies with a significant enhancement along Guinea Coast and a reduction over the west Sahel (not shown). Since the monsoon circulation is intensified and the rainfall over the west Sahel is reduced we believe that the subsidence induced by the Indian Ocean warming is the main cause of the rainfall decline. The induced subsidence over the west Sahel does not continue to the surface and therefore does not lead to an increase in geopotential height in the lower troposphere which could trigger a weaker monsoon circulation to west Africa. Thus the weakening of the west Sahel precipitation in our Indian Ocean experiment is caused by anomalous subsidence in the middle and upper troposphere and not by a reduction in the monsoonal circulation to west Africa.

The Atlantic plus Indian Ocean experiment shows a clear rainfall reduction over both areas—Guinea Coast and the west Sahel (Fig. 8d). It seems that the separate responses to both the Indian and the Atlantic SST anomalies can be combined to first order to explain the observed rainfall reduction over sub-Saharan west Africa in 1983 (Fig. 4). This study indicates that the warming in the Indian Ocean caused the rainfall reduction over the west Sahel and eastern tropical Atlantic SSTs the rainfall reductions along Guinea Coast. The difference between the superposition of rainfall anomalies in the separate Atlantic and the Indian Ocean experiments and those resulting from the combined Indian plus Atlantic Ocean experiment are not significant in most parts of sub-Saharan West Africa (not shown). We cannot rule out that the 21-year integration time of the simulations are not long enough to extract the non-linear effects, however, the superposition of the two separate experiments produces a too strong negative rainfall anomaly along the coast of west Africa compared to the combined experiment and a too weak negative rainfall anomaly in the eastern part of the west Sahel (east of 10°*W*).

6 Discussion and conclusions

In this paper, we have demonstrated that both Indian and eastern tropical Atlantic Ocean SSTs can play a significant role in forcing rainfall anomalies over sub-Saharan West Africa on inter-annual time scales and that just such a situation occurred during summer of 1983. We would be remiss if we did not point out that Indian Ocean SST anomalies observed during the summer of 1983 were highly unusual and that our results may only be useful in this context and should not be generalised. We do not imply that SST variability in the tropical Atlantic and Indian Ocean solely explains rainfall variability over sub-Saharan West Africa, but rather that the combined SST forcing can, at least in certain years, be an important driving force of sub-Saharan West Africa rainfall variability.

Pacific SST anomalies were not able to directly—via the atmosphere—force rainfall anomalies similar to those

observed in the summer of 1983 over sub-Saharan West Africa. The role of variability in tropical Pacific SSTs might be more indirect in this case—a strong El Niño event that was concentrated in the boreal winter of 1982 and spring of 1983 may have had a remanent effect on forcing the Indian Ocean SST anomalies observed in the summer of 1983 (Tourre and White 1995). Air-sea interaction in the Indian Ocean may be important in this respect (Webster et al. 1999). The SST anomalies in the eastern tropical Atlantic were probably paramount for the rainfall along Guinea Coast, whereas the Indian Ocean was instrumental in causing the drought over the Sahel during the summer of 1983. Colder SSTs in the eastern tropical Atlantic and the associated reduction in water vapour content of the lower troposphere seem to be the main cause of the rainfall reductions along Guinea Coast. The impact of Atlantic SST anomalies on West African rainfall during the boreal summer of 1983 seems to be meridional confined to approximately 10°*N*. Reductions in rainfall during the summer of 1983 north of this latitude were linked to changes in the large-scale atmospheric circulation resulting from an anomalously warm Indian Ocean. The warming in the Indian Ocean caused large scale subsidence in the middle and upper troposphere over West Africa that suppressed convection.

Our results may at a first glance seem to contradict previous results that suggest a link between eastern tropical Pacific SST anomalies and Sahelian rainfall. In our Pacific experiment the warming in the eastern equatorial Pacific is still appeared—a reminiscent of the 1982/1983 El Niño—, but the central Pacific had already cooled. The Pacific forcing used for example by Rowell (2001) is much stronger than in our experiments. Rowell showed a significant change in east Sahel rainfall but more or less no impact on the west Sahel (see Rowell's Fig. 6a) when using composite differences computed over El Niño-years minus La Nina-years. The weaker east Sahel rainfall response in our Pacific Ocean experiment may partly be explained by the weaker forcing.

Our findings concerning the mechanisms related to the reduction of the rainfall over the Sahel in the experiments for summer 1983 seem to be consistent with a revised description of the West African monsoon by Nicholson 2009. Analysing the NCEP/NCAR reanalysis data, she found that the surface ITCZ is effectively independent of the system that produces most of the rainfall over the Sahel. The primary mechanism of rain-production is the ascent lying between the AEJ and the TEJ. In our Indian Ocean experiment, rainfall reductions over the West Sahel are related to reduced ascent in the levels between the lower (AEJ) and upper-level (TEJ) jets. This paper strengthens the view that surface ITCZ variability is not necessarily related to the main rain-producing system over the Sahel.

Acknowledgments The authors would like to thank Serge Janicot, Nils Gunnar Kvamst Ivar Seierstad, Ellen Marie Viste and Justin Wettstein for their useful comments. We thank the Max-Planck-Institute for Meteorology for providing and supporting the ECHAM5 model. The UK Meteorological Office and Hadley Centre is acknowledged for providing the HadISST 1.1—global SST—data-set. This work was supported by the COMPAS and NOClim project funded by the research council of Norway and by the AMMA project of the European Union.

References

Bader J, Latif M (2003) The impact of decadal-scale Indian Ocean sea surface temperature anomalies on Sahelian rainfall and the North Atlantic Oscillation. Geophys Res Lett 30(22):2169. doi: 10.1029/2003GL018426.

Bretherton CS, Widmann M, Dymnikov VP, Wallace JM, Blade I (1999) The effective number of spatial degrees of freedom of a time-varying field. J Clim 12:1990–1999

Chiang JCH, Sobel AH (2002) Tropical tropospheric temperature variations caused by ENSO and their influence on the remote tropical climate. J Clim 15:2616–2631

Folland CK, Palmer TN, Parker DE (1986) Sahel rainfall and worldwide sea temperatures, 1901−85. Nature 320:602–607

Fontaine B, Janicot S, Moron V (1995) Rainfall anomaly patterns and wind field signals over West Africa in August (1958–1989). J Clim 8:1503–1510

Giannini A, Saravanan R, Chang P (2003) Oceanic forcing of Sahel rainfall on interannual to inter-decadal time scales. Science 302:1027–1030

Hastenrath S (1984) Interannual variability and annual cycle. Mechanism of circulation and climate in the tropical Atlantic sector. Mon Wea Rev 112:1097–1107

Janicot S (1992) Spatiotemporal variability of West African rainfall. Part I: Regionalizations and typings. J Clim 5:489–497

Janicot S, Moron V, Fontaine B (1996) Sahel droughts and ENSO dynamics. Geophys Res Lett 23:515–518

Janowiak JE (1988) An investigation of interannual rainfall variability in Africa. J Clim 1:240–255

Kalnay E, Kanamitsu M, Kistler R, Collins W, Deaven D, Gandin L, Iredell M, Saha S, White G, Woollen J, Zhu Y, Leetmaa A, Reynolds B, Chelliah M, Ebisuzaki W, Higgins W, Janowiak J, Mo KC, Ropelewski C, Wang J, Jenne R, Joseph D (1996) The NCEP/NCAR 40-Year Reanalysis Project. BAMS 77:437–471

Lamb PJ (1978a) Case studies of tropical Atlantic surface circulation patterns during recent sub-Saharan weather anomalies, 1967 and 1968. Mon Wea Rev 106:482–491

Lamb PJ (1978b) Large-scale tropical Atlantic surface circulation patterns associated with sub-Saharan weather anomalies. Tellus A30:240–251

Lamb PJ, and Peppler RA (1992) Further case studies of tropical Atlantic surface circulation patterns associated with sub-Saharan drought. J Clim 5:476–488

Latif M, Grötzner A (2000) The equatorial Atlantic oscillation and its response to ENSO. Clim Dyn 2–3:213–218

Lu J, Delworth TL (2005) Oceanic forcing of the late 20th century Sahel drought. Geophys Res Lett 32:L22706. doi:10.1029/2005GL023316

Lu J (2009) The dynamics of the Indian Ocean sea surface temperature forcing of Sahel drought. Clim Dyn 33:445–460. doi:10.1007/s00382-009-0596-6

Mitchell TD, Jones PD (2005) An improved method of constructing a database of monthly climate observations and associated high-resolution grids. Int J Climatol 25:693–712

New MG, Hulme M, Jones PD (2000) Representing twentieth-century space-time climate variability. Part II: Development of 1901–1996 monthly grids of terrestrial surface climate. J Clim 13:2217–2238

Newell RE, Kidson JW (1984) African mean wind changes between Sahelian wet and dry periods. J Clim 4:27–33

Nicholson SE (1980) The nature of rainfall fluctuations in subtropical West Africa. Mon Wea Rev 108:473–487

Nicholson SE, Palao IM (1993) A re-evaluation of rainfall variability in the Sahel. Part I: Characteristics of rainfall fluctuations. Int J Climatol 13:371–389

Nicholson SE (1997) An analysis of the ENSO signal in the tropical Atlantic and western Indian oceans. Int J Climatol 17:345–375

Nicholson SE, Grist JP (2001) A conceptual model for understanding rainfall variability in the West African Sahel on interannual and interdecadal timescales. J Climatol 21:1733–1757

Nicholson SE, Grist JP (2003) The seasonal evolution of the atmospheric circulation over West Africa and Equatorial Africa. J Clim 16:1013–1030

Nicholson SE (2009) A revised picture of the structure of the monsoon and land ITCZ over West Africa. Clim Dyn. doi: 10.1007/s00382-008-0514-3

Palmer TN (1986) Influence of the Atlantic, Pacific and Indian Oceans on Sahel rainfall. Nature 322:251–253

Rayner NA, Parker DE, Horton EB, Folland CK, Alexander LV, Rowell DP, Kent EC, and Kaplan A (2003) Global analyses of sea surface temperature, sea ice ,and night marine air temperature since the late nineteenth century. J Geophys Res Atmos 108(D14):4407. doi:10.1029/2002JD002670

Roeckner E, Bäuml G, Bonaventura L, Brokopf R, Esch M, Giorgetta M, Hagemann S, Kirchner I, Kornblueh L, Manzini E, Rhodin A, Schlese U, Schulzweida U, Tompkins A (2003) The atmospheric general circulation model ECHAM 5. MPI Report 349

Roeckner E, Brokopf R, Esch M, Giorgetta M, Hagemann S, Kornblueh L, Manzini E, Schlese U, Schulzweida U (2006) Sensitivity of simulated climate to horizontal and vertical resolution in the ECHAM5 atmosphere model. J Clim 19(16): 3771–3791. doi:10.1175/JCLI3824.1

Rowell DP (2001) Teleconnections between the tropical Pacific and the Sahel. Quart J Roy Meteor Soc 127:1683–1706

Rowell DP (2003) The impact of Mediterranean SSTs on the Sahelian rainfall season. J Clim 16:849–862

Schnitzler KG, Knorr W, Latif M, Bader J, Zeng N (2001) Vegetation feedback on Sahelian rainfall variability in a coupled climate land-vegetation model. MPI Report 329

Shinoda M, Kawamura R (1994) Tropical rainbelt, circulation, and sea surface temperatures associated with the Sahelian rainfall trend. J Meteorol Soc Jpn 72:341–357

Taylor KE, Williamson D, Zwiers F (2000) PCMDI Report 60

Tett SFB, Mitchell JFB, Parker DE, Allen MR (1996) Human influence on the atmospheric vertical temperature structure: detection and observations. Science 274:1170–1173

Tourre YM, White WB (1995) El Niño signals in the global upper-ocean temperature. J Phys Oceanagr 25:1317–1332

Vizy EK, Cook KH (2001) Mechanisms by which Gulf of Guinea and eastern North Atlantic sea surface temperature anomalies can influence African rainfall. J Clim 14:795–821

Vizy EK, Cook KH (2002) Development and application of a mesoscale climate model for the tropics: influence of sea surface temperature anomalies on the West African monsoon. J Geophys Res Atmos 107

Ward MN (1998) Diagnosis and short-lead time prediction of summer rainfall in tropical North Africa at interannual and multidecadal timescales. J Clim 11:3167–3191

Ward MN , Lamb PJ, Portis DH, el Hamly M, Sebbari R (1999) Climate variability in northern Africa. Understanding droughts in the Sahel and the Maghreb. In: Navarra A (ed) Beyond el Niño: decadal and interdecadal climate variability. Springer-Verlag, Berlin, pp 119–140

Webster PJ, Andrew MM, Johannes PL, Robert RL (1999) Coupled ocean-atmosphere dynamics in the Indian Ocean during 1997–98. Nature 401:356–360. doi:10.1038/43848

Xie P, Arkin PA (1996) Analyses of global monthly precipitation using gauge observations, satellite estimates, and numerical model predictions. J Clim 9:840–858

Zeng N, Neelin JD, Lau KM, Tucker CJ (1999) Enhancement of interdecadal climate variability in the Sahel by vegetation interaction. Science 286:1537–1540